JOURNAL OF PROPULSION AND POWER
Vol. 20, No. 3, May–June 2004

Three-Dimensional Multi-Objective Design Optimization of a Transonic Compressor Rotor

Ernesto Benini*
University of Padova, 35131 Padova, Italy

A method for transonic compressor multi-objective design optimization was developed and applied to the NASA rotor 37, a test case representative of complex three-dimensional viscous flow structures in transonic bladings. The optimization problem considered was to maximize the isentropic efficiency of the rotor and to maximize its pressure ratio at the design point, using a constraint on the mass flow rate. The three-dimensional Navier–Stokes code CFX-TASCflow® was used for the aerodynamic analysis of blade designs. The capability of the code was validated by comparing the computed results to experimental data available in the open literature from probe traverses up- and downstream of the rotor. A multi-objective evolutionary algorithm was used for handling the optimization problem that makes use of Pareto optimality concepts and implements a novel genetic diversity evaluation method to establish a criterion for fitness assignment. The optimal rotor configurations, which correspond to the maximum pressure ratio and maximum efficiency, were obtained and compared to the original design.

Nomenclature

m	=	distance along meridional curve, m
m'	=	radius-normalized distance along meridional curve
$\dot{m}$	=	mass flow rate, kg/s
p	=	pressure, Pa
$r, r\theta, z$	=	cylindrical coordinates, m
T	=	temperature, K
t	=	thickness, m
η_{is}	=	isentropic efficiency

Subscripts

choke	=	choking condition
0	=	total
1	=	inlet
4	=	outlet

Introduction

IN modern high-performance aircraft engines, compressor stages are required to operate with the highest values of both the efficiency and the compression ratio. This helps minimize the fuel consumption and decrease the engine weight and size due to the reduction in the number of stages and their cross-sectional area. Transonic compressors have been developed during the past three decades to achieve this goal. In these machines, the inner portion of the rotor blade operates at subsonic relative speeds, whereas in the outer part the flow is supersonic. This is a direct consequence of the high relative Mach numbers of the flow approaching the blade needed to obtain a high-compression ratio per single stage. The main drawback is that the rotors experience the existence of intense shock waves that are generated close to blade tip and over part of the span. It is well known that shock waves are responsible for high aerodynamic losses and entropy generation that negatively influence overall efficiency. At the same time, however, the shock determines a significant increment in the blade diffusion and, thus, contributes to achieving a high-compression ratio.

The presence of complex shock structures that interact with the main flow and wall boundary layers explains why the design of such machines is so challenging. In fact, the design principle is not to avoid shocks (as is the case in subsonic compressors), but to control their locations and strengths to achieve maximum performance. Computational fluid dynamics (CFD) is of practical importance for this purpose because it helps the designer to better understand the features of the flowfield and establish the way the geometry of the blade has to be designed and, if necessary, modified. Examples of CFD calculations on transonic compressor blades can be easily found in the open literature.[1–5] Navier–Stokes analyses, in particular, make it possible to deal with the real three-dimensional design problem and to study the effect of changes in the three-dimensional blade shape. These include both the application of high-performance airfoils for transonic bladings, as well the use of sweep and lean in blade radial stacking.[6–10]

CFD alone can be very useful in the framework of a conventional trial-and-error procedure of a transonic blade, but it becomes even more powerful when combined with an optimization technique. This aspect has recently been investigated by several researchers and the results documented in relevant publications. Lee and Kim[11] used a gradient-based method to optimize the blades of a compressor using the three-dimensional Navier–Stokes equations. Ahn and Kim[12] developed an optimization technique for the NASA rotor 37 based on the response surface method. Oyama et al.[13] used evolutionary algorithms in the redesign of the blade of NASA rotor 67. The latter was also adopted by Tiow and Zangeneh[14] as a test case for the application of a three-dimensional inverse design methodology. Tiow et al.[15] developed and applied an inverse design technique coupled with a simulated annealing optimization algorithm in the design of transonic axial blade cascades.

In all of the cited works, optimization and inverse methodologies were adopted to minimize aerodynamic losses. In the present work, a multi-objective optimization algorithm is applied with the aim of optimizing a transonic rotor blade with respect to both the aerodynamic efficiency and the pressure ratio. To achieve this goal, evolutionary algorithms[16] are preferred to deterministic algorithms in view of their ability to capture global optima and because of their intrinsic capability to support an optimization problem involving multiple objectives. The paper is organized in the following way: First, a brief summary on the influence of three-dimensional blade geometry on performance of transonic rotors is presented. This is done with the aim of giving a justification about the choice of the design parameters. Then, the multi-objective optimization problem with regard to NASA rotor 37 is formulated, and the optimization

Received 3 June 2003; presented as Paper 2003-4090 at the AIAA 16th Computational Fluid Dynamics Conference, Orlando, FL, 23 June 2003; revision received 13 October 2003; accepted for publication 13 October 2003. Copyright © 2003 by the American Institute of Aeronautics and Astronautics, Inc. All rights reserved. Copies of this paper may be made for personal or internal use, on condition that the copier pay the $10.00 per-copy fee to the Copyright Clearance Center, Inc., 222 Rosewood Drive, Danvers, MA 01923; include the code 0748-4658/04 $10.00 in correspondence with the CCC.

*Contract Professor, Department of Mechanical Engineering, Via Venezia, 1; ernesto.benini@unipd.it. Member AIAA.

tools used to deal with it are described. Finally, the results of the optimization are presented and discussed.

Influence of Blade Shape on Transonic Compressor Flows

Effect of Blade Profiles

At high-subsonic relative Mach numbers, some areas of supersonic flow appear on both the suction and the pressure surfaces. These areas are usually followed by shock waves, which interact with the profile boundary layer and often lead to its separation. Since the development of the first and second generation of controlled diffusion airfoils,[17,18] the knowledge regarding the design of shock-free or shock-controlled profiles has dramatically improved, and this has led to successful increments in stage efficiency, loading, and stall margin.

In blade profiles with a supersonic inlet flow, the greatest attention is directed toward the inlet region because it fixes the maximum mass flow capacity and produces the majority of the pressure rise.[19] Downstream of the inlet region, the flow is generally subsonic as a result of the presence of a passage shock, and therefore, the criteria usually employed for subsonic blading may be appropriate there to guide the designer toward achieving best performance. For a given operating point defined by the inlet Mach number and incidence angle, the behavior of the inlet region is defined by the loading distribution, particularly the position and magnitude of the peak load. Recently, this aspect has been very well described by Tiow et al.,[15] who demonstrated how a reduction in the peak load and the shift in its position from the rear to the front result in diminishing the intensity of the shock patterns. In the rear of the profile, the loading distribution is still regarded as very important and has to be carefully specified.[20]

Some recent achievements in the field of transonic compressor bladings, however, have shown that shock structure and strength cannot be controlled only by using a proper airfoil shape, but also by taking advantage of the shape of the radial stacking curve, in particular including three-dimensional lean and sweep.

Effect of Three-Dimensional Sweep and Lean

The concept of incorporating blade sweep for controlling shock structures and secondary flows has been largely documented in the literature.

In absence of shocks, sweep and lean are known to be effective in reducing the onset and development of secondary flows within a blade row. Yamaguchi et al.[21] tested, in particular, the effect of forward sweep and described a qualitative mechanism for suppressing secondary flows near the endwall region. They found that in forward-swept rotor blades the accumulation of low-momentum fluid near the endwall tip region is much lower than in conventional radial blades due to the decreasing radial migration of fluid particles within the boundary layer, a phenomenon that follows the imbalance between the centrifugal force and the pressure gradient.

In transonic compressors, the presence of shock structures further complicates the flow within the blades. Since the experience of Prince,[6] it has been recognized that a three-dimensional-shaped shock structure, as occurs in swept rotors, may be responsible for reduced shock losses. This would be the consequence of the formation of a less strong oblique shock wave in the spanwise direction compared to a high-strength normal shock, which is usually found in conventional transonic blades. Recently, Hah et al.[4] carried out an extensive experimental and numerical study on three transonic rotors (unswept, aft swept and forward swept) and found that the forward-swept rotor had a higher peak efficiency than the baseline unswept configuration, as well as 30% larger stall margin. However, the aft-swept rotor showed almost the same peak efficiency as the baseline rotor, but a reduction of about 40% in the stall margin.

The influence of blade lean in transonic compressor rotors has not been extensively described in the literature. Results of both experimental and numerical studies refer, in fact, to the effect of lean (often called dihedral) on subsonic linear cascades[22] and subsonic annular cascades (bowed stators).[23–26] However, the use of lean is currently exploited in axial-flow fan rotors.[27] The general guidelines that result from these studies are difficult to apply to transonic rotors because of the strong interaction between low-momentum fluid near the endwall and the shock waves. In a recent paper,[12] the use of negative tip dihedral (where the profile stacking curve is skewed toward the direction of rotation) was investigated numerically in a transonic rotor and the results showed a positive influence on the overall rotor efficiency.

Optimization of NASA Rotor 37

Rotor 37 designed at NASA John H. Glenn Research Center at Lewis Field, was selected for optimization because it is a well-documented test case, where strong interactions (such as corner stall, shock/boundary-layer, tip–vortex, and tip leakage secondary interactions) occur. Even though it was developed more than 20 years ago, rotor 37 is representative of design and performance levels of the most advanced transonic blades used today in gas turbine inlet stages. Some design information and overall stage performance came from Reid and Moore,[28] and detailed measurement data were provided by Moore and Reid.[29] The main dimensions of the rotor are given in Fig. 1.

The rotor has 36 multiple-circular-src (MCA) blades, inlet hub–tip diameter ratio of 0.7, blade aspect ratio of 1.19, and a tip solidity of 1.29. The running tip clearance is 0.0356 cm (0.45% of the blade span). The inner diameter increases in the mean flow direction, whereas the outer diameter decreases, and the blades are stacked in the radial direction in such a way that the flow shows typical three-dimensional features. Design performance at the nominal rotating speed of 17,188 rpm (at International Standards Organization conditions) as estimated during the design computations are the following: mass flow rate 20.19 kg/s, total pressure ratio 2.106, total temperature ratio 1.27, and adiabatic efficiency 0.877. The experimental maximum mass flow rate at the choking condition is 20.93 kg/s. The flow surveys were placed in stations 1 and 4 [Fig. 2, (Ref. 30)]. Cobra probes were used for total pressure and flow angle measurements, with a thermocouple for total temperature data; wedge probes were used for static pressure, and wall static pressure taps were employed on the hub and tip walls.

The purpose of the optimization considered here was to maximize the two-objective function:

$$\boldsymbol{F} = (\eta_{\mathrm{is}},\, p_{04}/p_{01}) \tag{1}$$

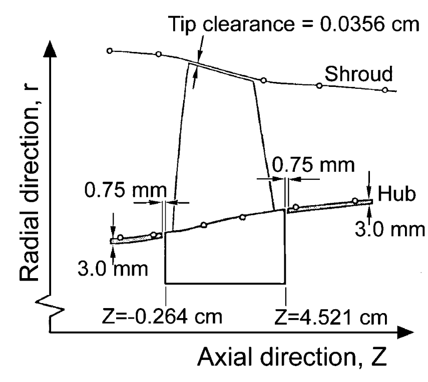

Fig. 1 Meridional geometry of NASA rotor 37, from AGARD.[30]

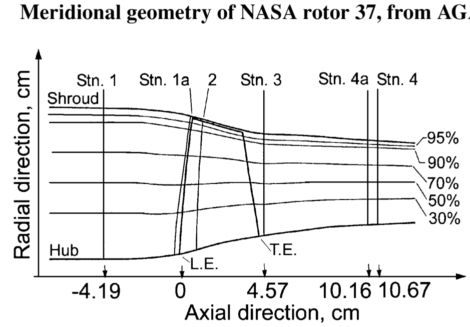

Fig. 2 Measurement stations within NASA rotor 37, from AGARD.[30]

where η_{is} is the adiabatic efficiency and p_{04}/p_{01} the total-to-total pressure ratio, both referred to stations 1 and 4 of Fig. 2. The optimization was conducted for one mass flow condition ($\dot{m}/\dot{m}_{choke} = 0.98$), this being one of the cases for which many of the experimental and computational results are available to the public. The inlet total pressure and total temperature were fixed at $p_{01} = 101325$ Pa and $T_{01} = 288.15$ K.

The optimization was carried out using an optimization method that integrates a code for three-dimensional blade geometry parameterization, a Navier–Stokes solver, and an optimization algorithm. A detailed description of this method, along with examples of its application to design optimization of turbomachinery blades may be found elsewhere.[20,31,32]

Blade Geometry Definition

To make the results of the optimization comparable to those regarding the baseline configuration, the meridional contours of the hub and casing were not modified. Actually, a change in the meridional area would have had a strong impact on the aerodynamic blockage and, therefore, on the compressor flow capacity.

The rotor blade geometry was parameterized using three profiles along the span (hub, midspan, and tip profiles), each of which was described by camber and thickness distributions (Fig. 3). These were defined by fourthorder Bezier polynomials, where only the values of the ordinates of the control points (θ for the camber line and t the thickness) were allowed to vary as independent design variables.

The blade surface was then obtained by the interpolation of profile coordinates in the span direction by use of spline curves. When a proper value of the θ coordinate of the first midspan and the tip profiles' control point with respect to the hub profile were specified the effect of blade lean was achieved. The use of blade sweep, on the other hand, which could be obtained in principle by giving a different z coordinate to the three profiles, was not investigated. The results of preliminary calculations indicated that, because the casing contour is fixed here, a forward-swept rotor would necessarily have a greater diameter and, therefore, would lead to higher aerodynamic losses caused by higher incidence tip Mach numbers. For the same reason, the chord distribution along the span was not changed compared to the original design.

A total of 14 parameters for the camber lines plus 9 parameters for the thickness distributions (the leading-edge and trailing-edge radii were not changed), that is, 23 parameters in total, were used to describe the three-dimensional shape of the rotor. Each parameter was given a range of variation. To avoid the creation of rotors having very different mass flow rates from that of the baseline configuration, the code that handled the blade parameterization calculated the geometric throat area between adjacent blades: Only the geometries that gave throat areas in the range of $\pm 0.2\%$ with respect the original geometry were then simulated, and the others were disregarded and eliminated before processing.

Flow Solver: Description and Validation

The CFD code CFX-TASCflow® was used to calculate the flowfield around the rotor, where the three-dimensional Reynolds-averaged Navier–Stokes equations are solved using a finite-element-based finite volume method. An algebraic multigrid method based on the additive correction multigrid strategy[33] was used along with the second order skew upwind differencing scheme with physical advection correction.[34]

The code was first validated against experimental data provided by Moore and Reid.[29] A multiblock structured grid of about 240,000 nodes per single passage (Fig. 4) was adopted following the guidelines provided in a recent AGARD report.[30] The flow region close to the profile wall was discretized using an O-type grid, whereas the outer part was meshed using an H-type grid. The effect of the tip clearance was also modeled. The k–ϵ turbulence model[35] along with standard wall functions were employed. The walls were treated as smooth and adiabatic. The boundary conditions were fixed as follows: At the domain inlet, the total pressure, total temperature, and flow angle were imposed; at the outlet, average static pressure was applied for both near-stall and near-choke conditions; periodic boundary conditions were imposed on the lateral faces of the flow domain. An angular velocity corresponding to the nominal rotational speed was applied to the rotor. The rotor performance was calculated over the entire operating range. For each simulation, the convergence criterion was established when normalized rms residuals were less than 5×10^{-7}. Each simulation took about 4 hours to complete on a Workstation AlphaServer ES40.

Results of the code validation are given in Fig. 5. With regard to overall performance, both the adiabatic efficiency and pressure ratio were slightly underestimated in all of the operating conditions. In particular, the pressure ratio seemed to have a dominant effect on the overall efficiency, as suggested by the radial plots, based on pitch-averaged data at station 4, in Fig. 5. In fact, in a large portion of the span the pressure ratio was lower than the measured one, and because the temperature ratio was predicted rather well, a lower value of the efficiency was calculated. This tendency seems to be in contrast with other published results[30] regarding a similar application of CFX-TASCflow, where the pressure ratio tended to be overpredicted in all of the conditions.

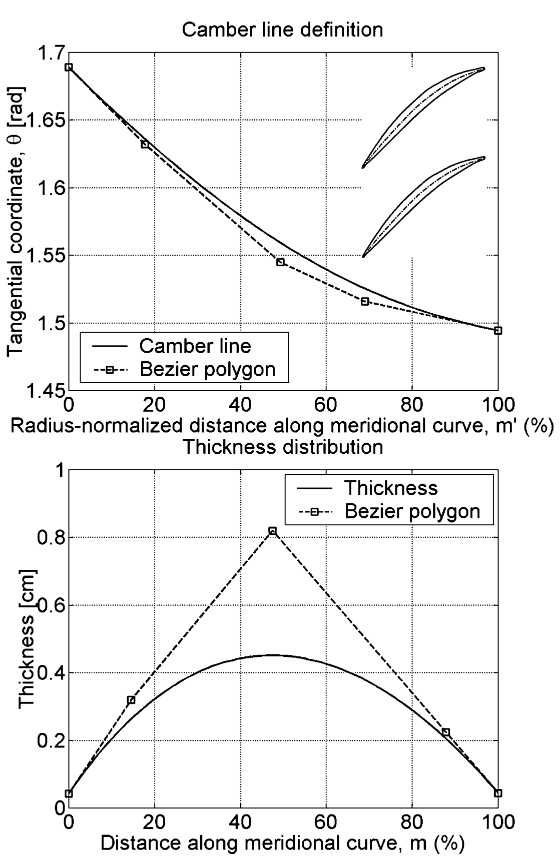

Fig. 3 Parameterization of a compressor airfoil.

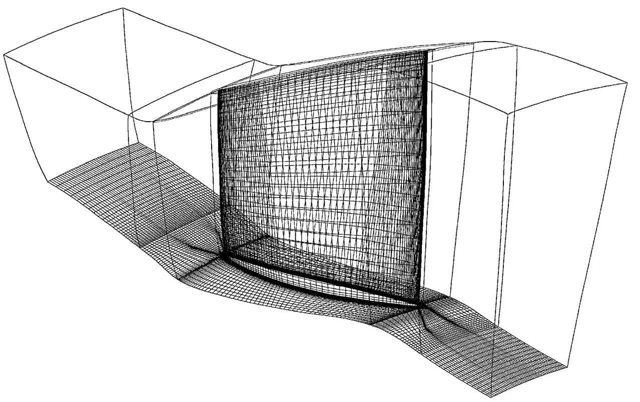

Fig. 4 Multiblock grid used in the simulations.

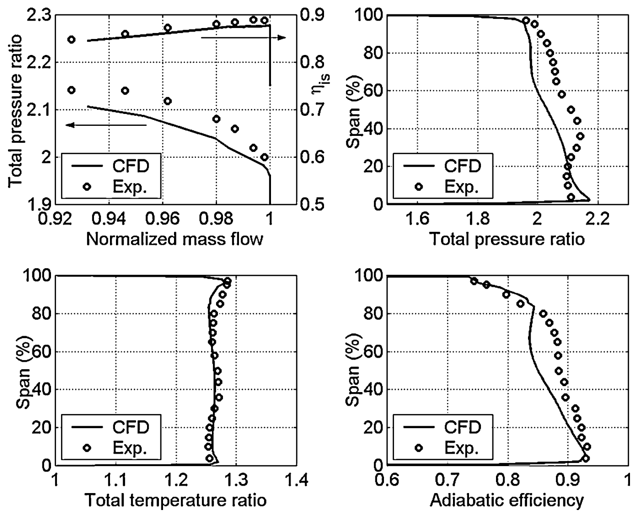

Fig. 5 Results of the code validation.

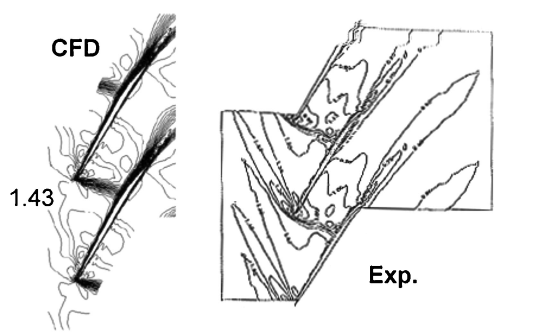

Fig. 6 Comparison between calculated and experimental Mach number contours at 90% span and $\dot{m}/\dot{m}_{choke} = 0.98$: maximum Mach = 1.576, minimum Mach = 0, and contour interval = 0.031.

Figure 6 shows the computational and experimental results of the relative Mach number contour plots at 90% span and 98% choke flow. The calculated shock position and resolution were quite good as a result of the alignment of the grid lines along the mean flow direction. The region where the passage shock and the boundary layer on the suction side of an adjacent blade intersect was calculated quite well, although the shock wave front seemed wider than the experimental one. Hildebrandt (see Ref. 30), showed that, to improve shock resolution, a grid of about 500,000 nodes, that is, finer than the one used here, should be used.

Multi-Objective Evolutionary Algorithm

Evolutionary algorithms[16] are optimization techniques that use both stochastic and deterministic elements, where an artificial evolution process that imitates the natural evolution of biological organisms is implemented. The evolution process starts with a randomly initialized population of individuals (a set of points in the search space) that evolves following the Darwinian principle of the survival of the fittest. According to this approach, new generations of solutions are created using some simulated evolutionary operators, such as crossover and mutation: The probability of survival for each individual depends on its fitness, that is, on how well it performs with respect to the objective(s) of the optimization problem. As a result, evolutionary algorithms are very well suited to deal with multi-objective problems because they make use of an evolving population of solutions that is driven toward the set of the true tradeoff among the objectives, the Pareto optimal set. For the same reason, they can be beneficially applied to highly multidimensional problems, where an effective exploration of the design space can be carried out only using populations with several individuals.

In this paper, the structure of the evolutionary algorithm follows the main steps of an evolution strategy and has been described in detail in previous papers.[20,36] After the parents are selected, reproduction using uniform crossover and mutation are performed to generate offspring that are then evaluated. The evaluation step includes reconstruction of rotor geometry from actual decision variables, CFD analysis with postprocessing, and ranking according to the usual Pareto concepts (see Ref. 16). Then a genetic diversity evaluation method (GeDEM) is applied to establish a criterion for fitness assignment and to build the next population of parents. In short, the GeDEM preserves genetic diversity of the best-so-far population of candidate solutions to the optimization problem by performing

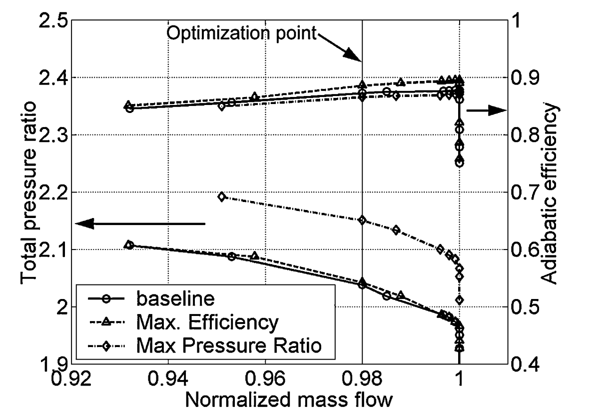

Fig. 7 Performance maps of the baseline and optimized configurations.

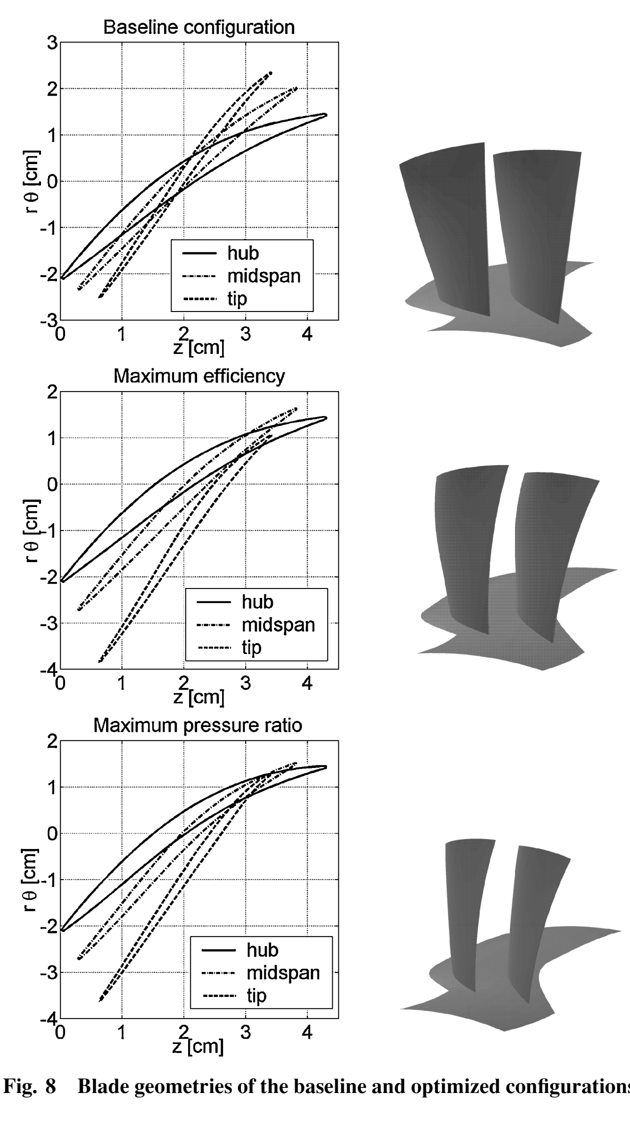

Fig. 8 Blade geometries of the baseline and optimized configurations.

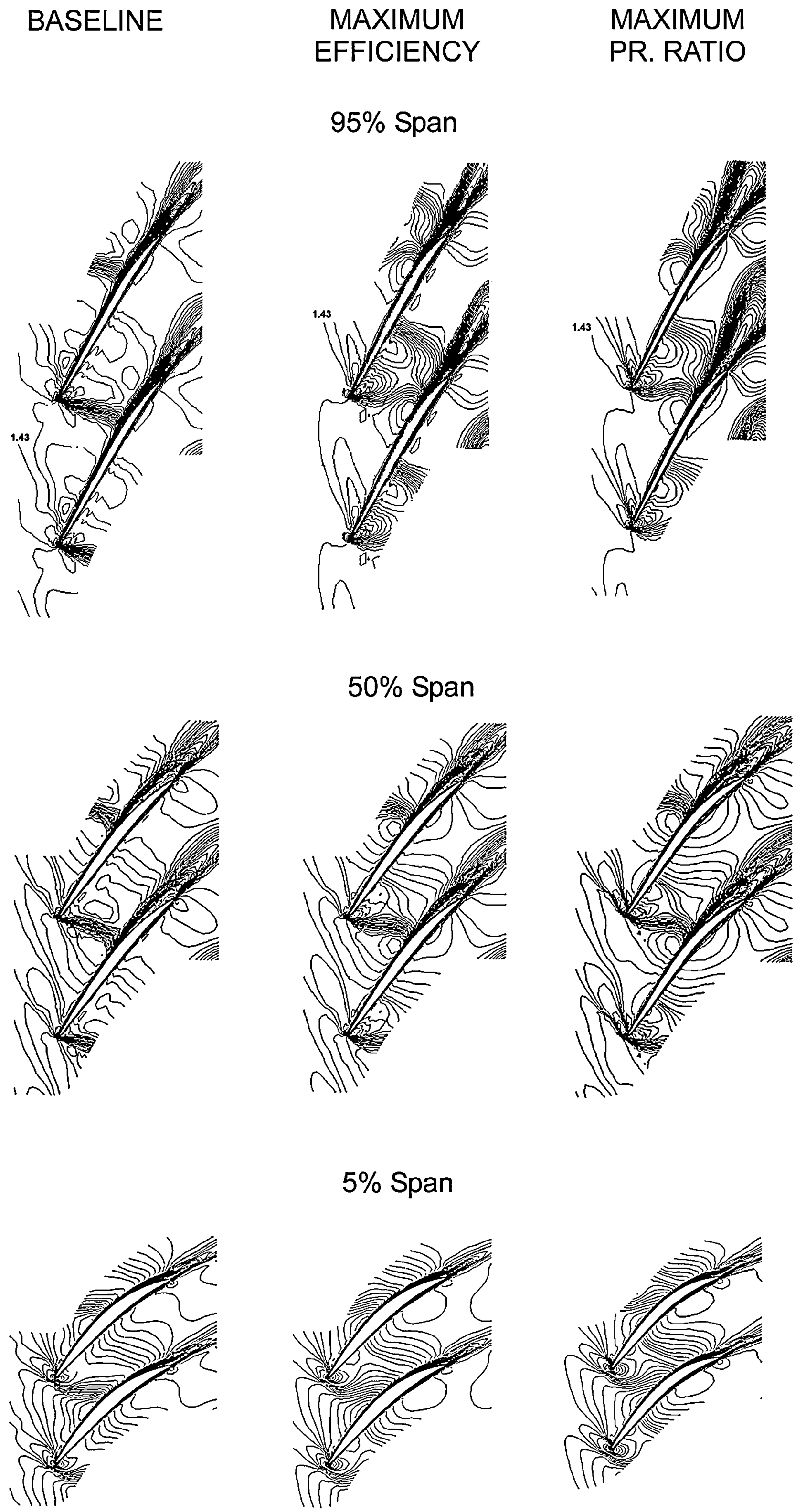

a) Maximum Mach = 1.576, minimum Mach = 0.0, and delta Mach = 0.031

b) Maximum Mach = 1.583, minimum Mach = 0.0, and delta Mach = 0.031

c) Maximum Mach = 1.595, minimum Mach = 0.0, and delta Mach = 0.031

Fig. 9 Mach number contours at 95, 50, and 5% span of baseline and optimized geometries.

an additional evaluation after the common measure of objective fitness. This evaluation ranks the solutions according to their fitness value and their reciprocal distance as a way to give more reproduction chances to both highly fit and highly distant individuals. The loop starts again until the predetermined number of generations has elapsed.

Results

During the optimization run, a population of 20 individuals evolved for a total of 100 generations. Computations were performed in parallel on a four-processor Workstation AlphaServer ES40 and the overall turn around time was about 2000 h. Because of time constraints, it was not possible to continue the computations further. A mass flow rate boundary condition at the outlet was applied to each configuration examined during the evolutionary process to fix the condition $\dot{m}/\dot{m}_{\text{choke}} = 0.98$.

Figure 7 shows the results of the optimization, that is, the performance of optimized configurations with respect to both maximum efficiency and maximum pressure ratio. These configurations correspond to the borders of the final Pareto front obtained after the optimization. In fact, in the objective function space, the performance of the optimized individuals was very much clustered around the original as a result of the tight constraint imposed on the mass flow rate, which prevented the search algorithm from generating and evaluating geometries very different from the original design.

At the chosen optimization point, an improvement in the adiabatic efficiency was achieved (+1.5% with respect to the original geometry) without modifying the pressure ratio. On the other hand, an optimal individual was obtained that showed a higher pressure ratio (+5.5%) with a slightly smaller efficiency (−0.8%) compared to the original design. This behavior was observed over the entire operating range of the compressor (Fig. 7). In fact, for nearly the same pressure ratio, the efficiency-optimized (E-O) rotor definitely showed a superior efficiency close to the choking condition ($\Delta\eta_{\text{is}} = +2\%$). Moreover, the operating range was very similar to the original one. The pressure ratio-optimized (PR-O) rotor had instead a smaller operating range compared to the original one. The last computation for which the CFD code was able to reach convergence occurred at $\dot{m}/\dot{m}_{\text{choke}} = 0.951$, which perhaps denotes the stall limit.

The geometries of the optimized configurations are compared with the original design in Fig. 8. The main differences could be found in both profile shape and radial stacking. Changes in the profile shape concerned the region close to the trailing edge, as one might expect, because the constraint on the geometrical throat area led to cascade geometries having very similar inlet regions. The E-O rotor had profiles (particularly the one located close to blade tip) with an increased thickness toward the rear and a different curvature. Furthermore, the blade profiles leaned significantly in the direction of rotation. This result confirms the one obtained by Ahn and Kim,[12] even if the amount of leaning was considerably higher here (+1.5 deg compared to +0.22 deg). The impact of this lean on the structural strength of the blade should, therefore, be checked carefully. The PR-O blade was characterized by higher cambered profiles toward the rear, with no noticeable changes in the thickness distribution compared to the original design. (An exception was the profile at midspan, where the maximum thickness is slightly lower.) Again the blade leaned substantially in the direction of rotation, even if in a less apparent way compared to the E-O blade.

The effect of blade shape changes on rotor performance can be better understood by examining the contours of the Mach number reported in Fig. 9. From Fig. 9, it appears that in the E-O blade the shock intensity was reduced close to blade tip as the shock wave moved from a nearly normal to a much more oblique pattern. Actually, the normal shock wave at the tip was substituted by two oblique shocks of lesser intensity, whereas at midspan the shock still weakened and became more oblique to the incoming flow. This is also confirmed by Fig. 10, where a comparison of the Mach number contours near the suction surface for the three blades is given. In the original configuration, a strong shock wave occurred within the blade passage that turned normal to the casing and led to high

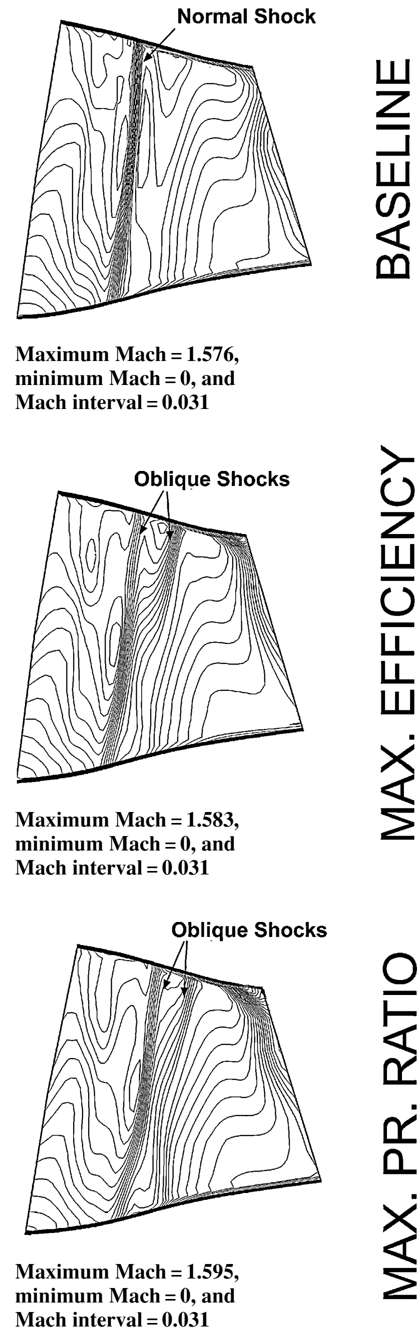

Fig. 10 Mach number contours on the suction surface of the baseline and optimized blades.

aerodynamic losses and severe shock/boundary-layer interaction. In both the E-O and PR-O blades, the shock bifurcated into two less-severe branches and almost vanished into two shock/boundary-layer interaction zones. In the E-O blade, this led to higher efficiency, whereas in the PR-O blade the concomitant effect of an increased blade profile curvature, which helped to achieve a high-pressure ratio, resulted in a more evident boundary-layer separation toward the rear and, therefore, in a lesser overall efficiency. In addition, this is the reason why the PR-O blade achieved a smaller operating range: The blade was no longer capable of effectively withstanding flow deviation at reduced incidence angles without incurring in massive separations (stall) toward the rear.

Conclusions

A method for three-dimensional multi-objective optimization of a transonic rotor blade was developed and tested which was based on an evolutionary algorithm and a Navier–Stokes code. The method was applied to the design optimization of NASA rotor 37 with the aim of achieving maximum efficiency and maximum pressure ratio with a constraint on the mass flow rate. The rotor blade was described using three profiles along the span, each of which was defined using parametric curves. The effect of blade lean was considered by changing the mutual tangential coordinates of the three profiles.

The optimization run was carried out on a multi-processor computer and demonstrated that the overall adiabatic efficiency can be improved by approximately 1.5% (without changing the pressure ratio in a significant way) by giving the blade a proper lean toward the direction of rotation and by slightly changing the profile shape, especially toward the tip. This improvement followed from a drastic modification in the shock structure within the blade passage. The results also showed that the improvement in the overall efficiency, achieved in one operating point, is maintained at off-design conditions.

The results also showed that the pressure ratio can be improved by about 5.5% by paying for a small efficiency drop (−0.8%). This was achieved by leaning the blade in the direction of rotation and by slightly increasing the profile curvature toward the rear to assure a subsonic diffusion. In this case, however, the presence of a shock wave, although less intense, accentuated the interaction between the shock and the boundary layer on the rear of the suction surface, a phenomenon that possibly determined a reduction in the operating range of the compressor.

Acknowledgments

The author is indebted to João Amaral Teixeira of Cranfield University (United Kingdom) for his valuable suggestions regarding simulations of NASA Rotor 37.

References

[1]Miller, D. P., and Bryans, A. C., "The Relative Merits of Inviscid Euler 3D and Quasi-3D Analysis for Design of Transonic Rotors," American Society of Mechanical Engineers, ASME Paper 88-GT-69, 1988.

[2]Hah, C., and Wennerstrom, A. J., "Three-Dimensional Flow Fields inside a Transonic Compressor with Swept Blades," *Journal of Turbomachinery*, Vol. 113, No. 1, 1991, pp. 241–251.

[3]Bassi, F., Rebay, S., and Savini, M., "Transonic and Supersonic Inviscid Computations Using Adaptive Unstructured Meshes," American Society of Mechanical Engineers, ASME Paper 91-GT-312, 1991.

[4]Hah, C., Puterbaugh, S. L., and Wadia, A. R., "Control of Shock Structure and Secondary Flow Field Inside Transonic Compressor Rotors Through Aerodynamic Sweep," American Society of Mechanical Engineers, ASME Paper 98-GT-561, 1998.

[5]Copenhaver, W. W., Mayhew, E. R., Hah, C., and Wadia, A. R., "The Effect of Tip Clearance on a Swept Transonic Compressor Rotor," *Journal of Turbomachinery*, Vol. 118, No. 1, 1995, pp. 230–239.

[6]Prince, D. C. J., "Three-Dimensional Shock Structures for Transonic/Supersonic Compressor Rotors," *Journal of Aircraft*, Vol. 17, No. 1, 1980, pp. 28–37.

[7]Wennerstrom, A. J., "Experimental Study of a High-Through-Flow Transonic Axial Compressor Stage," *Journal of Engineering for Gas Turbines and Power*, Vol. 106, No. 3, 1984, pp. 552–560.

[8]Neubert, R. J., Hobbs, D. E., and Weingold, H. D., "Application of Sweep to Improve the Efficiency of a Transonic Fan, Part 1: Design," AIAA Paper 90-1915, 1990.

[9]Wadia, A. R., Szucs, P. N., and Crall, D. W., "Inner Workings of Aerodynamic Sweep," American Society of Mechanical Engineers, ASME Paper 97-GT-401, 1997.

[10]Hah, C., Puterbaugh, S. L., and Wadia, A. R., "A Critical Evaluation of a Three-Dimensional Navier Stokes Method as a Tool to Calculate Transonic Flows inside a Low-Aspect-Ratio Compressor," *CFD Techniques for Propulsion Applications*, CP-510, AGARD, 1991.

[11]Lee, S. Y., and Kim, K. Y., "Design Optimization of Axial Flow Compressor Blades with Three-Dimensional Navier–Stokes Solver," American Society of Mechanical Engineers, ASME Paper 2000-GT-0488, 2000.

[12]Ahn, C.-S., and Kim, K.-Y., "Aerodynamic Design Optimization of an Axial Compressor Rotor," American Society of Mechanical Engineers, ASME Paper GT-2002-30445, 2002.

[13]Oyama, A., Liou, M.-S., and Obayashi, S., "Transonic Axial-Flow Blade Shape Optimization Using Evolutionary Algorithm and Three-Dimensional Navier–Stokes Solver," AIAA Paper 2002-5642, 2002.

[14]Tiou, W. T., and Zangeneh, M., "Application of a Three-Dimensional Viscous Transonic Inverse Method to NASA Rotor 67," *Journal of Power and Energy*, Vol. 216, No. 3, 2002, pp. 243–255.

[15]Tiou, W. T., Yiu, K. F. C., and Zangeneh, M., "Application of Simulated Annealing to Inverse Design of Transonic Turbomachinery Cascades," *Journal of Power and Energy*, Vol. 216, No. 1, 2002, pp. 59–73.

[16]Deb, K., *Multi-Objective Optimization Using Evolutionary Algorithms*, Wiley, Chichester, England, U.K., 2001.

[17]Hobbs, D. E., and Weingold, H. D., "Development of Controlled Diffusion Airfoils for Multistage Compressor Applications," *Journal of Engineering for Gas Turbines and Power*, Vol. 106, No. 1, 1984, pp. 271–278.

[18]Behlke, R. F., "The Development of a Second Generation of Controlled Diffusion Airfoils for Multistage Compressors," *Journal of Turbomachinery*, Vol. 108, No. 1, 1986, pp. 32–41.

[19]Cumspty, N. A., *Compressor Aerodynamics*, Longman Group UK, London, 1989.

[20]Benini, E., and Toffolo, A., "Development of High-Performance Airfoils for Axial Flow Compressors Using Evolutionary Computation," *Journal of Propulsion and Power*, Vol. 18, No. 3, 2002, pp. 544–554.

[21]Yamaguchi, N., Tominaga, T., Hattori, S., and Mitsubishi, T., "Secondary-Loss Reduction by Forward-Skewing of Axial Compressor Rotor Blading," *Proceedings of 1991 Yokohama International Gas Turbine Congress*, Vol. 2, 1991.

[22]Breugelmans, F. A. E., Carels, Y., and Demuth, M., "Influence of Dihedrail on the Secondary Flow in a Two Dimensional Compressor Cascade," *Journal of Engineering for Gas Turbine and Power*, Vol. 106, No. 3, 1984, pp. 578–584.

[23]Wisler, D. C., "Loss Reduction in Axial-Flow Compressors Through Low-Speed Model Testing," *Journal of Engineering for Gas Turbines and Power*, Vol. 107, No. 2, 1985, pp. 354–363.

[24]Robinson, C. J., Northall, J. D., and McFarlane, C. W. R., "Measurement and Calculation of the Three-Dimensional Flow in Axial Compressor Stators With and Without Endbends," American Society of Mechanical Engineers, ASME Paper 89-GT-6, 1989.

[25]Schultze, H. D., Gallus, H. E., and Lakshminarayana, B., "Three-Dimensional Separated Flow Field in the Endwall Region on an Annular Compressor Cascade in the Presence of Rotor-Stator Interaction: Part I—Quasi-Steady Flow Field and Comparison with Steady State Data," *Journal of Turbomachinery*, Vol. 112, No. 4, 1990, pp. 669–678.

[26]Weingold, H. D., Neubert, R. J., Behlke, R. F., and Potter, G. E., "Bowed Stators: An Example of CFD Applied to Improve Multistage Compressor Efficiency," *Journal of Turbomachinery*, Vol. 119, No. 1, 1997, pp. 161–168.

[27]Cai, N., and Xu, J., "Aerodynamic-Aeroacoustic Performance of Parametric Effects for Skewed-Swept Rotor," American Society of Mechanical Engineers, ASME Paper 2001-GT-0354, 2001.

[28]Reid, L., and Moore, R. D., "Design and Overall Performance of Four Highly Loaded, High-Speed Inlet Stages for an Advanced High-Pressure-Ratio Core Compressor," NASA TP 1337, 1978.

[29]Moore, R. D., and Reid, L., "Performance of Single-Stage Axial Flow Transonic Compressor With Rotor and Stator Aspect Ratios of 1.19 and 1.26, Respectively, and With Design Pressure Ratio of 2.05," NASA TP 1659, 1980.

[30]"CFD Validation for Propulsion System Components," AGARD-ar-355, AGARD, May 1998.

[31]Benini, E., "Optimal Navier Stokes Design of Compressor Impellers Using Evolutionary Computation," *International Journal of Computational Fluid Dynamics* (to be published).

[32]Benini, E., and Toffolo, A., "A Parametric Method for Optimal Design of Two-Dimensional Cascades," *Journal of Power and Energy*, Vol. 215, No. A4, 2001, pp. 465–473.

[33]Hutchinson, B. R., and Raithby, G. D., "A Multigrid Method Based on Additive Correction Strategy," *Numerical Heat Tranfer*, Vol. 9, No. 5, 1986, pp. 511–537.

[34]Raw, M. J., Galpin, P. F., and Hutchinson, B. R., "A Colocated Finite Volume Method for Solving the Navier–Stokes Equations for Compressible Flows in Turbomachinery: Results and Applications," *Canadian Aeronautics and Space Journal*, Vol. 35, 1989, pp. 189–196.

[35]Launder, B., and Spalding, D., "Numerical Computation of Turbulent Flows," *Computer Methods in Applied Mechanics and Engineering*, Vol. 3, No. 2, 1974, pp. 269–289.

[36]Toffolo, A., and Benini, E., "Genetic Diversity as an Objective in Multi-Objective Evolutionary Algorithms," *Evolutionary Computation*, Vol. 11, No. 2, 2003, pp. 151–167.